Faster responses of photosynthesis to light transitions increase biomass and grain yield in transgenic *Sorghum bicolor* overexpressing Rieske FeS

Maria Ermakova[1], Russell Woodford[1], Zachary Taylor[1,2], Robert T. Furbank[1], Srinivas Belide[3], Susanne von Caemmerer[1]

[1] Centre of Excellence for Translational Photosynthesis, Division of Plant Science, Research School of Biology, The Australian National University, Acton, 2601 ACT, Australia.

[2] Max Planck Institute of Molecular Plant Physiology, Potsdam, Brandenburg, Germany.

[3] CSIRO Food & Agriculture, Canberra, ACT, Australia.

*Corresponding author: Maria Ermakova, maria.ermakova@anu.edu.au.

Maria Ermakova, maria.ermakova@anu.edu.au, ORCID: 0000-0001-8466-4186

Russell Woodford, Russell.Woodford@anu.edu.au, ORCID: 0000-0002-6766-2274

Zachary Taylor, taylor@mpimp-golm.mpg.de, ORCID: 0000-0002-7396-4893

Robert T. Furbank, robert.furbank@anu.edu.au, ORCID: 0000-0001-8700-6613

Srinivas Belide, Srinivas.Belide@csiro.au, ORCID: 0000-0001-9536-8200

Susanne von Caemmerer, Susanne.Caemmerer@anu.edu.au, ORCID: 0000-0002-8366-2071

Keywords (6-10): sorghum, crop yield, C_4 photosynthesis, light interception, electron transport, photosynthesis induction.

Abstract

Sorghum is one of the most important crops providing food and feed in many of the world's harsher environments. Sorghum utilises the C_4 pathway of photosynthesis in which a biochemical carbon concentrating mechanism results in high CO_2 assimilation rates. Overexpressing the Rieske subunit of the Cytochrome b_6f complex was previously shown to increase the rate of photosynthetic electron transport and stimulate CO_2 assimilation in the model C_4 plant *Setaria viridis*. To test whether productivity of C_4 crops could be improved by Rieske overexpression, we created transgenic *Sorghum bicolor* plants with increased Rieske content. The transgenic plants showed no marked changes in abundance of other photosynthetic proteins or chlorophyll content. Increases in yield of Photosystem II and CO_2 assimilation rate as well as faster responses of non-photochemical quenching during transient photosynthetic responses were observed as a result of an elevated *in vivo* Cytochrome b_6f activity in plants overexpressing Rieske. The steady-state rates of electron transport and CO_2 assimilation did not differ between transgenic and control plants, suggesting that Cytochrome b_6f is not the only factor limiting electron transport in sorghum at high light and high CO_2. Nevertheless, more agile responses of photosynthesis to light transitions led to increases in biomass and grain yield in plants overexpressing Rieske. Our results indicate that increasing Rieske content could boost productivity of C_4 crops by improving the efficiency of light utilisation and conversion to biomass.

Introduction

C_4 plants utilise a specialised photosynthetic pathway in which a metabolic C_4 cycle acts as a biochemical carbon concentrating mechanism (Hatch, 1987). The C_4 cycle operates between mesophyll and bundle sheath (BS) cells, and Ribulose-1,5-bisphosphate carboxylase/oxygenase (Rubisco), the main enzyme of CO_2 fixation, is localised to the BS (Kanai and Edwards, 1999). Atmospheric CO_2 (in the form of HCO_3^-) is first fixed in mesophyll cells by PEP carboxylase (PEPC) into a C_4 acid (hence the term C_4 photosynthesis). C_4 acids diffuse to BS cells where they are decarboxylated to produce pyruvate and CO_2, providing high CO_2 partial pressure (pCO_2) around Rubisco (Furbank and Hatch, 1987). Higher carboxylation efficiency of Rubisco in C_4 plants allows higher radiation use efficiency and increased biomass production compared to C_3 plants (Long, 1999; Sage and Zhu, 2011). Because of their superior productivity, C_4 crops are becoming increasingly important for food and bioenergy security. The global production of C_4 maize (*Zea mays*) often surpasses the two key C_3 cereals, wheat and rice, and C_4 miscanthus (*Miscanthus* × *giganteus*) and switchgrass (*Panicum virgatum*) are two of the currently leading dedicated biomass crops. This has created

considerable interest in identifying and testing strategies to improve productivity of C_4 crops (Sales et al., 2021; von Caemmerer and Furbank, 2016).

While C_4 plants are more productive, running the C_4 cycle requires additional input of energy. Whilst C_3 plants need at least two NADPH and three ATP to fix one mol of CO_2, C_4 plants need two additional ATP molecules to regenerate PEP from pyruvate in mesophyll cells (Edwards et al., 2001; Hatch, 1987). NADPH and ATP are the products of light reactions of photosynthesis which include electron and proton transport in the thylakoid membranes of chloroplasts. NADPH is produced during linear electron flow as electrons originating from water split by Photosystem II (PSII) are transferred by the chain of cofactors, via Cytochrome *b*$_6$*f* complex (Cyt*b*$_6$*f*) and Photosystem I (PSI), to $NADP^+$. Cyt*b*$_6$*f* links oxidation of plastoquinol with the translocation of protons to the lumen, a space enclosed by the thylakoid membrane, by operating the Q-cycle (Malone et al., 2021). The transmembrane proton gradient (ΔpH) established across the thylakoid membrane creates a proton motive force (*pmf*) that drives ATP synthesis via the ATP synthase complex. In addition to linear electron flow, C_4 plants run active cyclic electron flow to produce additional ATP (Ishikawa et al., 2016; Munekage and Taniguchi, 2016; Nakamura et al., 2013). Cyclic electron flow returns electrons from the reducing side of PSI back to the plastoquinone (PQ) pool to repeat plastoquinol oxidation by Cyt*b*$_6$*f* and build up additional *pmf* (Johnson, 2011). Thus, cyclic electron flow results in the net production of ATP but not NADPH. ΔpH controls PSII activity by regulating the energy-dependent and quickly reversible form of non-photochemical quenching (NPQ) (Li et al., 2002). The latter is a common term for diverse reactions that help to reduce excitation energy reaching reaction centers of PSII (Malnoë, 2018). Establishing energy-dependent NPQ requires the PsbS protein that senses luminal pH and modifies the light-harvesting complex II (LHCII) to dissipate a part of absorbed light as heat, as well as the conversion of violaxanthin to zeaxanthin (Johnson et al., 2009; Li et al., 2004).

The vast majority of agriculturally important C_4 crops, like maize, sorghum (*Sorghum bicolor*), sugarcane, miscanthus and several millets (*e.g.*, *Setaria italica*), belong to the NADP-ME subtype of C_4 photosynthesis which employs $NADP^+$-dependent malic enzyme to decarboxylate the C_4 acid malate in BS chloroplasts (Furbank, 2011). Because of the drastic differences in biochemistry of mesophyll and BS cells in NADP-ME plants, electron transport chains of the two cell types are also largely different: mesophyll cells predominantly run linear electron flow and BS cells – cyclic electron flow (Ermakova et al., 2021a; Munekage, 2016). To coordinate the production of NADPH and ATP between cells, plants need to tightly regulate the distribution of available light energy (Bellasio and Ermakova, 2021; Bellasio and Lundgren, 2016). Because of their higher ATP requirement, C_4 plants generally require higher solar radiation and are typically found in tropical regions (Sage et al., 2011). At low irradiance however, slow operation of the C_4

cycle results in a lower pCO_2 in BS cells decreasing the efficiency of C_4 photosynthesis (Furbank and Hatch, 1987; Kromdijk et al., 2010). Therefore, increasing radiation use efficiency is one of the primary strategies for increasing assimilation rates and productivity of C_4 plants.

Constitutive overexpression of the Rieske FeS subunit of Cytb_6f (hereafter Rieske), encoded by the nuclear *petC* gene was shown to increase abundance of the whole complex in both mesophyll and BS cells of a model NADP-ME grass *Setaria viridis* (Ermakova et al., 2019). This resulted in a higher quantum yield of both photosystems and higher CO_2 assimilation rates at high light and high CO_2. However, the feasibility of using Rieske overexpression for improving crop productivity required further assessment. Here we test effects of Rieske overexpression on biomass and grain yield of a multipurpose C_4 crop, sorghum. We show that sorghum plants with increased Rieske abundance use light more efficiently and accumulate more biomass due to faster responses of photosynthesis to light transitions. Our results indicate that increasing Rieske content is a promising strategy for stimulating yield of sorghum and other C_4 crops.

Results

Sorghum plants transformed with the construct for Rieske overexpression (see Materials and Methods for details) were selected based on kanamycin resistance and transferred to soil for growth in a glasshouse. Sixteen T_0 plants were recovered and analysed for insertion number, transgene expression and leaf Rieske abundance. The *ntpII* insertions and transcripts of *Brachipodium dystachion petC* (*BdpetC*) were confirmed in ten T_0 plants (Fig. 1a and Fig. 1b). Plants 25, 26, 29 and 32 showed relatively higher Rieske abundance per leaf area compared to wild type (WT) and escape plants without the T-DNA insertion (Fig. 1a). The T_1 progenies of those four plants were grown and analysed for insertion numbers and Rieske abundance. The homozygous T_1 plants of lines 25 and 26 (4 insertions, Fig. 1c) had higher Rieske leaf content compared to control plants (WT and null segregants). Furthermore, homozygous plants 25-11 and 26-11 showed relatively lower NPQ compared to control and other T_1 plants when assayed at ambient light, in line with the NPQ phenotype reported in *S. viridis* overexpressing Rieske (Ermakova et al., 2019). The progenies of those two plants, as well as the progeny of the homozygous T_1 plant 32-14 with increased Rieske abundance (Fig. S1), were used in further experiments, and are hereafter referred to as transgenic lines 25, 26 and 32.

T_2 plants of the three transgenic lines and azygous control plants were grown over summer in a glasshouse with natural light. Abundance of photosynthetic proteins was analysed in leaf extracts loaded on leaf area basis by immunoblotting with specific antibodies (Fig. 2a). Quantification of immunoblots demonstrated a significant, about 40%, increase of Rieske content in all three transgenic lines compared to control plants. Relative abundance of other electron transport components, such as the D1 protein of PSII, AtpB subunit

of ATP synthase, PsbS and Lhcb2 subunit of LHC II was largely unaltered in transgenic plants overexpressing Rieske (Fig. 2b) as well as the relative Chl content (Table 1). The content of PEPC and Rubisco large subunit (RbcL) did not differ between transgenic and control plants (Fig. 2b).

Sorghum plants with increased Rieske content were taller than the control plants at 5 weeks after germination (Fig. 2c and Fig. 2d) and had more tillers ($0.036 < P > 0.09$, Table 1) and leaves (Fig. 2e). Whilst the leaf thickness and leaf dry mass per area did not differ between the genotypes (Table 1), the total aboveground biomass of lines 26 and 32 at harvest was higher compared to control plants (Fig. 2f). In another experiment, when plants were grown in a glasshouse during late summer-autumn, Rieske-OE plants of lines 25 and 26 had larger leaves compared to control plants (azygous and WT, Fig. S2) and produced more seeds by weight and number than control plants (Fig. 2g and Fig. 2h).

Next, we analysed photosynthetic properties of sorghum plants overexpressing Rieske. First, we conducted gas exchange and fluorescence analysis at different pCO_2 and irradiances. No significant differences in CO_2 assimilation rate or the effective yield of PSII (PhiPSII) were detected between the plants overexpressing Rieske and control plants at constant irradiance of 1500 µmol m^{-2} s^{-1} and different pCO_2 (Fig. 3, left panels). At ambient pCO_2, CO_2 assimilation rates and stomatal conductance were similar between the genotypes at all irradiances (Fig. 3, right panels). The photochemical and non-photochemical yields of PSI and PSII analysed at different irradiances were largely unaltered in transgenic plants compared to control plants (Fig. 4), except for the yield of PSI (PhiPSI) being higher and the non-photochemical loss of PSI yield due to the acceptor side limitation (PhiNA) being lower in lines 25 and 32 at 95 µmol m^{-2} s^{-1}. These results indicated that the steady-state rates of electron transport and CO_2 assimilation were largely not affected in plants overexpressing Rieske. The maximum quantum efficiency of PSII (F_V/F_M), however, was significantly higher in plants of line 32 compared to control plants (Table 1).

Energisation properties of the thylakoid membranes were tested by recording electrochromic shift signal and absorbance changes at 535 nm. By the end of 3-min illumination intervals, *pmf* and proton conductivity of the thylakoid membrane (g_{H+}), reflecting the speed of *pmf* dissipation and thus ATP synthase activity, did not differ between the plants overexpressing Rieske and control plants at any irradiance (Fig. 5a and Fig. 5b). To gain information about the kinetics of ΔpH build-up during the illumination, we recorded absorbance changes at 535 nm which reflect both zeaxanthin formation and the LHCII modifications induced by PsbS, therefore, providing information on the response of NPQ to ΔpH (Horton et al., 1991; Li et al., 2004). All three transgenic lines overexpressing Rieske established NPQ significantly faster than

control plants in the beginning of illumination upon the shift from dark to 1600 µmol m^{-2} s^{-1}, indicating a transiently faster build-up of ΔpH due to the increased Cytb_6f activity (Fig. 5c).

Since transient increase of Cytb_6f activity could be detected upon changes in illumination, we analysed the induction of photosynthesis in overnight-dark-adapted plants during the first 30 min of illumination with actinic light of 1000 µmol m^{-2} s^{-1} (Fig. 6). Because the steady-state CO_2 assimilation rate, PhiPSII and NPQ did not differ between genotypes (Fig. 3 and Fig. 4), we normalised these parameters to minimum and maximum values to facilitate comparison of the kinetics. During the induction of photosynthesis, CO_2 assimilation rates increased faster in sorghum plants overexpressing Rieske compared to control plants, and between 18 and 26 min the rates were significantly higher in all three transgenic lines. The induction kinetics of PhiPSII was similar to the kinetics of CO_2 assimilation rate. Transgenic lines reached the steady-state faster and lines 25 and 26 had significantly increased PhiPSII between 18 and 26 min since the beginning of illumination, compared to control plants (Fig. 6). Interestingly, during the first 9 min of illumination plants overexpressing Rieske built-up NPQ faster than control plants (significant in line 25 and 26) and line 32 then relaxed NPQ significantly faster. Importantly, although the stomatal conductance was significantly higher in all three lines overexpressing Rieske (Fig. 6d), increased CO_2 assimilation rates were not caused by an increased CO_2 availability since the ratio of intercellular to ambient CO_2 partial pressures (C_i/C_a) was unaltered (Fig. 6).

Discussion

Sorghum is one of the most important crops in the world which serves as a source of food, fodder and fuel. Sorghum can withstand severe droughts allowing it to grow in regions where other major crops cannot be grown, like Sub-Saharan Africa. However, in recent years, genetic progress in sorghum yield has stagnated and not kept pace with increasing demand (Ananda et al., 2020). Therefore, it is critical to develop new approaches for increasing sorghum productivity. Based on crop model predictions, up to 10% improvement in sorghum yield could be harnessed from improving photosynthesis (Wu et al., 2019). According to the biochemical model of C_4 photosynthesis, assimilation at low pCO_2 is limited by PEPC and CA activities and mesophyll conductance to CO_2, whilst assimilation at ambient and high pCO_2 is limited by Rubisco, electron transport or the regeneration rate of Rubisco's substrate (von Caemmerer, 2000; von Caemmerer, 2021; von Caemmerer and Furbank, 1999). Contribution of some of these factors to C_4 photosynthesis and plant productivity was recently tested using transgenic approach in the model C_4 plant *S. viridis* (Alonso-Cantabrana et al., 2018; Ermakova et al., 2022; Osborn et al., 2016), and improvements of C_4 photosynthesis were shown in *S. viridis* and *Z. mays* with increased Rieske and Rubisco content (Ermakova et al., 2019;

Ermakova et al., 2021b; Salesse-Smith et al., 2018). Here we expand on our previous results and assess how Rieske overexpression affects productivity of sorghum.

Rieske overexpression in sorghum provided increased Cytb_6f activity, confirmed by monitoring the build-up of NPQ and dynamics of electron transport during the photosynthesis induction. A faster build-up of NPQ during dark-light transition in transgenic plants indicated larger ΔpH due to increased Cytb_6f activity (Fig. 5c). Observing this transient increase is possible because NPQ engages on the scale of seconds to minutes (Müller et al., 2001). However, by the end of 3-min illumination periods, *pmf*, which is a sum of ΔpH and Δψ (the membrane potential), did not differ between genotypes (Fig. 5a). This was consistent with the largely unchanged electron transport parameters and CO_2 assimilation rates (Fig. 3 and Fig. 4) – all indicating that steady-state rates of electron transport were unaltered in sorghum plants overexpressing Rieske. Similar observations were made with tobacco plants overexpressing Rieske (Heyno et al., 2022). In C_3 plants, this phenomenon could be explained by a conserved relationship between ΔpH and NPQ which would reduce PSII activity in case if electron transport rate exceeds the capacity of dark reactions of photosynthesis to consume ATP and NADPH, typically due to a limited availability of CO_2 (Kanazawa and Kramer, 2002). C_4 photosynthesis, however, is less limited by CO_2 due to the C_4 cycle concentrating CO_2 around Rubisco, and an increase of electron transport rate is projected to provide proportional increase in assimilation (von Caemmerer and Furbank, 2016). Increasing Rieske content in *S. viridis* was sufficient to enhance electron transport rates, resulting in higher photosynthesis at non-limiting CO_2 and high light (Ermakova et al., 2019). One possible explanation for the difference observed between *S. viridis* and sorghum overexpressing Rieske is that C_4 crops underwent a selection for photosynthetic traits which could have altered a balance between electron transport components. For example, translational efficiency of Lhca6, a subunit of the light-harvesting complex I that facilitates a formation of PSI supercomplex involved in cyclic electron flow (Otani et al., 2018), was significantly enhanced during maize domestication (Zhu et al., 2021). Changes to the ratio of cyclic to linear electron flow likely resulted in additional or different factors limiting electron transport. Better understanding of photosynthetic changes that C_4 crops underwent during domestication will help to uncover additional targets for accelerating steady-state electron transport and photosynthesis rates (Hu et al., 2018; Tao et al., 2020a; Zhu et al., 2021). Increased assimilation rates detected in maize with increased Rubisco content at non-limiting CO_2 and high light could also be indicative of an altered relationship between electron transport and Rubisco limitations in C_4 crops (Salesse-Smith et al., 2018).

Interestingly, the largest difference in electron transport and assimilation between plants overexpressing Rieske and control plants was detected during the induction of photosynthesis. Induction, or activation of

photosynthesis during dark-to-light transition, is a complex process that, in C_3 plants, requires opening of stomata, activation of Rubisco and other enzymes and a build-up of metabolite concentrations (Deans et al., 2019; Slattery et al., 2018). Faster activation of photosynthesis was identified as one of the desirable traits in crop plants that could allow up to 20% increase in total assimilation (Acevedo-Siaca et al., 2020; Long et al., 2022). Activation of C_4 photosynthesis is further complicated by the distribution of electron transport and metabolic reactions between mesophyll and BS cells and a necessity to coordinate activities of C_4 and C_3 cycles (Furbank and Taylor, 1995; Kromdijk et al., 2014). Our results support previous works suggesting that, due to the operation of carbon concentrating mechanism, activation of C_4 photosynthesis is less limited by stomatal conductance compared to C_3 photosynthesis (Furbank and Walker, 1985; Usuda and Edwards, 1984). Indeed, in our experiments, C_i/C_a never dropped below 0.25 (Fig. 6e) which is equivalent to $C_i \geq 100$ µmol mol^{-1} sufficient to saturate assimilation (Pignon and Long, 2020). Instead, the observed increase of CO_2 assimilation rates during the light-induced activation of photosynthesis in sorghum overexpressing Rieske was underpinned by the higher PhiPSII (Fig. 6). It is conceivable that activation of photosynthetic enzymes provides a strong sink for ATP and NADPH, and an increased Cytb_6f activity could transiently stimulate electron transport to activate enzymes and build-up metabolite gradients faster. In line with this, activation of Rubisco that uses ATP was suggested as one of the major factors limiting C_4 photosynthesis during the induction (Wang et al., 2021).

Sorghum plants with increased Rieske content had increased biomass and grain yield. Transgenic plants produced more leaves and had larger leaves during the vegetative growth phase and accumulated more biomass by the end of growth season, compared to control plants (Fig. 2, Fig. S2). Moreover, transgenic plants produced about 20% more grain by weight and number (Fig. 2g and Fig. 2h) indicating that higher yield of transgenic plants was largely attributed to setting more seeds. Grain yield and grain number highly correlate in sorghum, and a supply of assimilates during the seed setting largely determines grain number (Craufurd and Peacock, 1993; van Oosterom and Hammer, 2008). Although the conditions of induction experiment (Fig. 6) were designed to maximise differences between control and transgenic plants and did not occur in glasshouse conditions, a cumulative effect of transiently or marginally increased electron transport rates could explain the observed improvements in biomass and yield of transgenic plants. Similarly, small changes in CO_2 assimilation rates due to accelerated NPQ relaxation were shown to result in significant increase in biomass of tobacco grown in the field (Kromdijk et al., 2016). Taken together, our results show that increasing Rieske content in sorghum improves the light use efficiency and stimulates biomass production therefore presenting a promising trait to be introduced into commercial sorghum

varieties. Exploring variation of Rieske content in sorghum variety panels (Tao et al., 2020b) could inform breeding programs for developing higher yielding sorghum with improved photosynthesis.

Conclusion

In sorghum, effects of Rieske overexpression on stimulating electron transport were more apparent during transient photosynthetic responses suggesting that other photosynthetic components co-limit the steady-state electron transport rate. However, faster responses of electron transport and CO_2 assimilation to light transients resulted in plants overexpressing Rieske accumulating more biomass and producing more grain. Our results indicate that increasing Rieske content, relative to other electron transport components, is a promising way to boost productivity of C_4 crops and ensure food and energy security.

Materials and Methods

Generation and selection of transgenic plants

The gene construct for Rieske overexpression was created using the Golden Gate cloning system (Engler et al., 2014), as described in Ermakova et al. (2019). The first expression module containing the selection marker was occupied by *neomycin phosphotransferase II* (*ntpII*) driven by the *Z. mays ubiquitine1* promotor. The second expression module contained the coding sequence of *petC* from *Brachipodium dystachion* (*BdpetC*) under the control of the *Z. mays ubiquitine1* promotor. The construct was transformed into *Agrobacterium tumefaciens* strain AGL1 and then into *Sorghum bicolor* Tx430 according to (Gurel et al., 2009). Transgenic plants were analysed for the *ntpII* copy number by digital PCR (iDNA genetics, Norwich, UK). Azygous plants were used as control in all experiments. Transcript abundance of *BdpetC* was estimated by qPCR as described in Ermakova et al. (2019). Electron transport at ambient light intensity and leaf properties (relative chlorophyll and leaf thickness) were assayed with MultispeQ (Kuhlgert et al., 2016) and analysed using the PhotosynQ platform (https://photosynq.com).

Plant growth conditions

Plants were grown in a glasshouse at ambient irradiance, 28 °C day, 20 °C night and 60% humidity. Plants were shuffled every 2-3 days to reduce any positional growth effects. The youngest fully expanded leaves of the 4-5 weeks old plants were used for all physiological analyses. Photos of plants, leaves and tiller count and height measurements were done during the fully emerged leaves stage, 5 weeks after germination.

Gas exchange and fluorescence analyses

Rates of CO_2 assimilation were measured over a range of pCO_2 and irradiance using a portable gas-exchange system LI-6800 (LI-COR Biosciences, Lincoln, NE). Chlorophyll fluorescence was assessed simultaneously with a Fluorometer head 6800-01 A (LI-COR Biosciences). Leaves were first equilibrated at 400 ppm CO_2 in

the reference side, 1500 µmol m^{-2} s^{-1}, leaf temperature 28 °C, 60% humidity and flow rate 500 µmol s^{-1}. CO_2 response curves were conducted under the constant irradiance of 1500 µmol m^{-2} s^{-1} by imposing a stepwise increase of pCO_2 from 0 to 1600 ppm at 3 min intervals. Light response curves were measured at the constant pCO_2 of 400 ppm in the reference cell under a stepwise decrease of irradiance from 0 to 2000 µmol m^{-2} s^{-1} at 3 min intervals. Red-blue actinic light (90%/10%) was used in all measurements. The effective yield of PSII (PhiPSII) was assessed at the end of each step upon the application of a multiphase saturating pulse (8000 µmol m^{-2} s^{-1}) and calculated according to Genty et al. (1989).

Induction of photosynthesis was analysed on dark-adapted overnight plants. First, leaves were clipped into LI-6800 chamber in darkness and the minimum and maximum levels of fluorescence were recorded upon the application of a saturating pulse. After that, leaves were illuminated with actinic light of 1000 µmol m^{-2} s^{-1}, and gas-exchange and fluorescence parameters were recorded every 1 min for 30 min. NPQ was calculated according to Bilger and Björkman (1990). All parameters were normalised for min and max values to facilitate comparison of the kinetics.

Electron and proton transport

Fluorescence parameters informing on the activity of PSII and absorbance at 820 nm reflecting the formation of oxidised P700, the reaction centre of PSI, were analysed simultaneously by the Dual-PAM-100 (Heinz Walz, Effeltrich, Germany). Measurements were done using red actinic light and 300-ms saturating pulses of 10000 µmol m^{-2} s^{-1}. Leaves were first dark-adapted for 30 min to record the minimal and maximal levels of fluorescence and calculate F_V/F_M, the maximum quantum yield of PSII. Then, a saturating pulse was applied after a pre-illumination with strong far-red light to record the maximal level of $P700^+$ signal and, after the pulse, the minimal level of $P700^+$ signal. Next, leaves were illuminated for 10 min with an actinic light of 378 µmol m^{-2} s^{-1}. After that, photosynthetic parameters were assessed over a range of irradiances from 0 to 2043 µmol m^{-2} s^{-1} at 2 min intervals by applying a saturating pulse at the end of each step. The effective quantum yield of PSII (PhiPSII), the yield of non-photochemical quenching (PhiNPQ) and the yield of non-regulated non-photochemical reactions within PSII (PhiNO) were calculated according to Kramer et al. (2004). The effective quantum yield of PSI (PhiPSI), the non-photochemical yield of PSI caused by the donor side limitation (PhiND) and the non-photochemical yield of PSI caused by the acceptor side limitation (PhiNA) were calculated according to Klughammer and Schreiber (2008).

The electrochromic shift signal (ECS) was monitored as the absorbance change at 515-550 nm using the Dual-PAM-100 equipped with the P515/535 emitter-detector module (Heinz Walz). The absorbance signal at 535 nm was monitored simultaneously. Leaves were first dark-adapted for 40 min and the amplitude of ECS induced by a single turnover flash was recorded. Dark-interval relaxation kinetics of ECS was then

recorded after 3-min intervals of illumination with red actinic light of increasing irradiance. Proton motive force (*pmf*) was estimated from the amplitude of the rapid decay of ECS signal upon light-dark transition, normalised for the ECS induced by the single turnover flash. Proton conductivity of the thylakoid membrane through ATP synthase was calculated as an inverse time constant obtained by the fitting of first-order ECS relaxation kinetics after Sacksteder and Kramer (2000).

Protein isolation and Western blotting

Total protein extracts were isolated from 0.7 cm^2 frozen leaf discs as described in Ermakova et al. (2019) and separated by SDS-PAGE. Proteins were then transferred to a nitrocellulose membrane and probed with antibodies against various photosynthetic proteins in dilutions recommended by the producer: Rieske (AS08 330, Agrisera, Vännäs, Sweden), D1 (Agrisera, AS10 704), PGR5 (Agrisera, AS163985). Quantification of immunoblots was performed with Image Lab software (Biorad, Hercules, CA).

Statistical analysis

The relationship between mean values of different groups was tested by one-way ANOVAs with Dunnett's or Tukey's *post-hoc* test or by two-tailed heteroscedastic *t*-test, as indicated in figure legends.

Acknowledgements

We thank Spencer Whitney for the gift of RbcL antibody and Siena Mitchell, Alexandra Williams, Ayla Manwaring, Kelly Chapman and James Samuel Nix for technical assistance. This work was performed under the collaborative project agreement between the Australian National University and CSIRO Food & Agriculture and supported by the Australian Research Council Centre of Excellence in Translational Photosynthesis (CE140100015) and by the seed grant from the Research School of Biology at the Australian National University. Authors declare no conflict of interests.

Author Contributions

SvC, ME and RTF designed the research; SB generated transgenic plants; ME, RW, SB and ZT performed research; ME and RW analyzed data; ME wrote the paper.

Short legends for Supporting Information

Fig. S1. Immunodetection of Rieske in the T_1 progeny of line 32.

Fig. S2. Length and width of top fully expanded leaves from WT, azygous and Rieske overexpressing plants.

Figure legends

Fig. 1. Selection of transgenic sorghum lines overexpressing Rieske. **a**. Immunodetection of Rieske in leaves of T_0 plants. **b**. Transcript abundance of *B. dystachion petC* (*BdpetC*) in T_0 sorghum plants. **c**. Immunodetection of Rieske in T_1 progenies of lines 25 and 26. (**a** and **c**) Samples were loaded on leaf area basis, and the titration series of WT samples was used for relative quantification. Insertion numbers indicate a copy number of *ntpII* obtained by digital PCR. Asterisks indicate the plants which progenies were used in further experiments. **d**. Quantum yield of non-photochemical quenching (PhiNPQ) measured at ambient irradiance in T_1 progenies of lines 25 and 26. WT and azygous plants were used as control. Each point represents a technical replicate.

Fig. 2. Protein analysis and growth of sorghum lines overexpressing Rieske. **a**. Immunodetection of photosynthetic proteins in leaves of control and transgenic plants: Rieske (Cytb_6f), D1 (PSII core), AtpB (ATP synthase), PsbS (energy-dependent non-photochemical quenching), Lhcb2 (light-harvesting complex II), RbcL (large subunit of Rubisco), PEPC (PEP carboxylase). Samples were loaded on leaf area basis, and the titration series of the Control sample #1 was used for relative quantification. **b**. Quantification of immunoblots relative to control plants. Mean ± SE, n = 3 biological replicates. **c.** Phenotype of plants 5 weeks after germination. (**d**, **e**, **f**) Height, leaf number and plant biomass, n = 5 biological replicates. (**g, h**) Total weight and number of seeds produced per plant, n = 18 biological replicates for Control (WT and azygous plants), n = 20 for Rieske-OE (lines 25 and 26). Asterisks indicate statistically significant differences between transgenic and control plants based on one-way ANOVA or t-test (**$P < 0.05$ or *$P < 0.1$).

Fig. 3. Gas exchange and fluorescence analysis of control and transgenic sorghum plants overexpressing Rieske at different pCO_2 (left panels, measured at 1500 µmol photons m^{-2} s^{-1}) or irradiance (right panels, measured at ambient pCO_2). PhiPSII, the effective quantum yield of PSII; gsw, stomatal conductance to water vapor. Azygous plants were used as control. Mean ± SE, n = 5 biological replicates. No statistically significant differences were found between transgenic and control plants (one-way ANOVA and Dunnett's post-hoc test at $P < 0.05$).

Fig. 4. Electron transport parameters estimated at different irradiance from leaves of control and transgenic sorghum plants overexpressing Rieske. PhiPSII, the effective quantum yield of PSII; PhiNPQ, the yield of non-photochemical quenching; PhiNO, the yield of non-regulated non-photochemical reactions within PSII; PhiPSI, the effective quantum yield of PSI; PhiND, the non-photochemical yield of PSI due to the donor side limitation; PhiNA, the non-photochemical yield of PSI due to the acceptor side limitation. Azygous plants were used as control. Mean ± SE, n = 5 biological replicates. Asterisks indicate statistically significant

difference between line 25 (black) or line 32 (grey) and control plants (one-way ANOVA and Dunnett's post-hoc test at $P < 0.05$).

Fig. 5. Analysis of the thylakoid membrane energisation in control plants and transgenic sorghum lines overexpressing Rieske. (**a** and **b**) Proton motive force (*pmf*) and proton conductivity of the thylakoid membrane (g_{H+}) at different irradiance analysed using electrochromic shift signal. Mean ± SE, n = 4 biological replicates. **c**. Absorbance changes at 535 nm recorded upon the shift from dark to 1600 µmol m^{-2} s^{-1}. The absorbance at the beginning and end of the 3-min illumination period was normalised to 0 and 1, respectively, to facilitate comparison of the kinetics. Averages of 4 biological replicates are presented. Azygous plants were used as control. Asterisks indicate intervals of statistically significant difference between transgenic and control plants (one-way ANOVA and Dunnett's post-hoc test at $P < 0.05$).

Fig. 6. Induction of photosynthesis during the first 30 min of illumination with actinic light of 1000 µmol m^{-2} s^{-1} in control plants and transgenic sorghum lines overexpressing Rieske. PhiPSII, the effective quantum yield of PSII; NPQ, non-photochemical quenching; gsw, stomatal conductance to water vapor; C_i/C_a, the ratio between the intercellular and ambient CO_2 partial pressures. The values of each parameter, except for C_i/C_a, at the beginning and end of the 30-min illumination were normalised to 0 and 1, respectively, to facilitate comparison of the kinetics. Azygous plants were used as control. Mean ± SE, n = 5 biological replicates. Asterisks indicate intervals of statistically significant differences between transgenic and control plants (one-way ANOVA and Dunnett's post-hoc test at $P < 0.05$).

382 **Table 1**. Properties of control plants and transgenic sorghum lines overexpressing Rieske. Azygous plants
383 were used as control. Mean ± SE, *n* = 5 biological replicates. Asterisks indicate statistically significant
384 differences between transgenic and control plants (one-way ANOVA and Dunnett's *post-hoc* test at
385 $P < 0.05$). LMA, leaf mass per area; F_V/F_M, the maximum quantum efficiency of PSII.

	Control	Line 25	Line 26	Line 32
Relative Chl	60.1 ± 1.9	57.6 ± 1.9	60.9 ± 1.8	60.5 ± 1.8
Leaf thickness, mm	0.63 ± 0.05	0.63 ± 0.03	0.60 ± 0.03	0.63 ± 0.04
LMA, g (dry weight) m^{-2}	119.42 ± 4.78	115.73 ± 4.08	113.92 ± 4.72	122.32 ± 2.65
Tiller number, $plant^{-1}$	1.4 ± 0.27	2.4 ± 0.45	2.0 ± 0.36	2.0 ± 0.36
F_V/F_M	0.802 ± 0.002	0.802 ± 0.006	0.803 ± 0.003	0.810 ± 0.001*

386

387

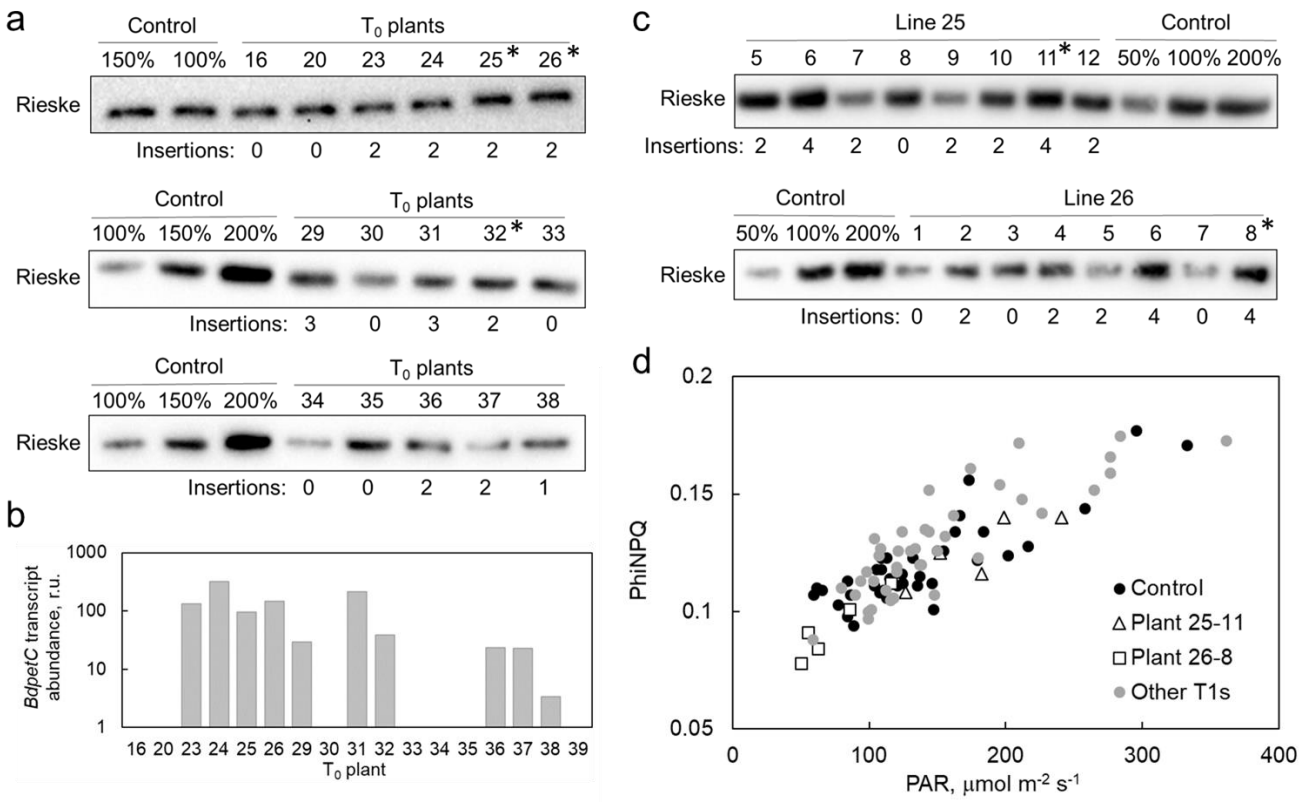

Fig. 1. Selection of transgenic sorghum lines overexpressing Rieske. **a**. Immunodetection of Rieske in leaves of T_0 plants. **b**. Transcript abundance of *B. dystachion petC* (*BdpetC*) in T_0 sorghum plants. **c**. Immunodetection of Rieske in T_1 progenies of lines 25 and 26. (**a** and **c**) Samples were loaded on leaf area basis, and the titration series of WT samples was used for relative quantification. Insertion numbers indicate a copy number of *ntpII* obtained by digital PCR. Asterisks indicate the plants which progenies were used in further experiments. **d**. Quantum yield of non-photochemical quenching (PhiNPQ) measured at ambient irradiance in T_1 progenies of lines 25 and 26. WT and azygous plants were used as control. Each point represents a technical replicate.

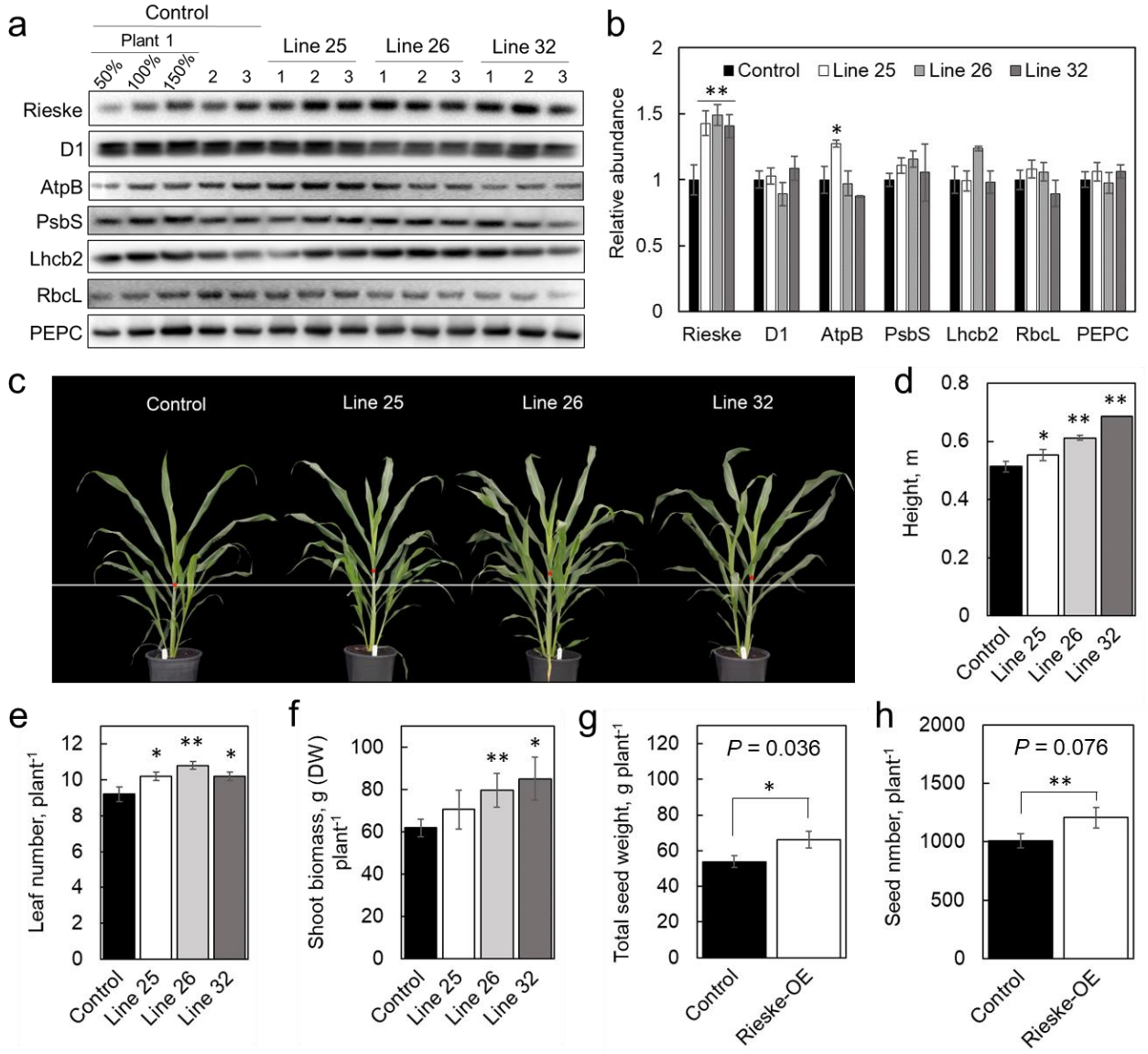

399

400 **Fig. 2.** Protein analysis and growth of sorghum lines overexpressing Rieske. **a**. Immunodetection of
401 photosynthetic proteins in leaves of control and transgenic plants: Rieske (Cytb_6f), D1 (PSII core), AtpB (ATP
402 synthase), PsbS (energy-dependent non-photochemical quenching), Lhcb2 (light-harvesting complex II),
403 RbcL (large subunit of Rubisco), PEPC (PEP carboxylase). Samples were loaded on leaf area basis, and the
404 titration series of the Control sample #1 was used for relative quantification. **b**. Quantification of
405 immunoblots relative to control plants. Mean ± SE, *n* = 3 biological replicates. **c.** Phenotype of plants 5
406 weeks after germination. (**d**, **e**, **f**) Height, leaf number and plant biomass, *n* = 5 biological replicates. (**g, h**)
407 Total weight and number of seeds produced per plant, *n* = 18 biological replicates for Control (WT and
408 azygous plants), *n* = 20 for Rieske-OE (lines 25 and 26). Asterisks indicate statistically significant differences
409 between transgenic and control plants based on one-way ANOVA or *t*-test (**$P < 0.05$ or *$P < 0.1$).

410

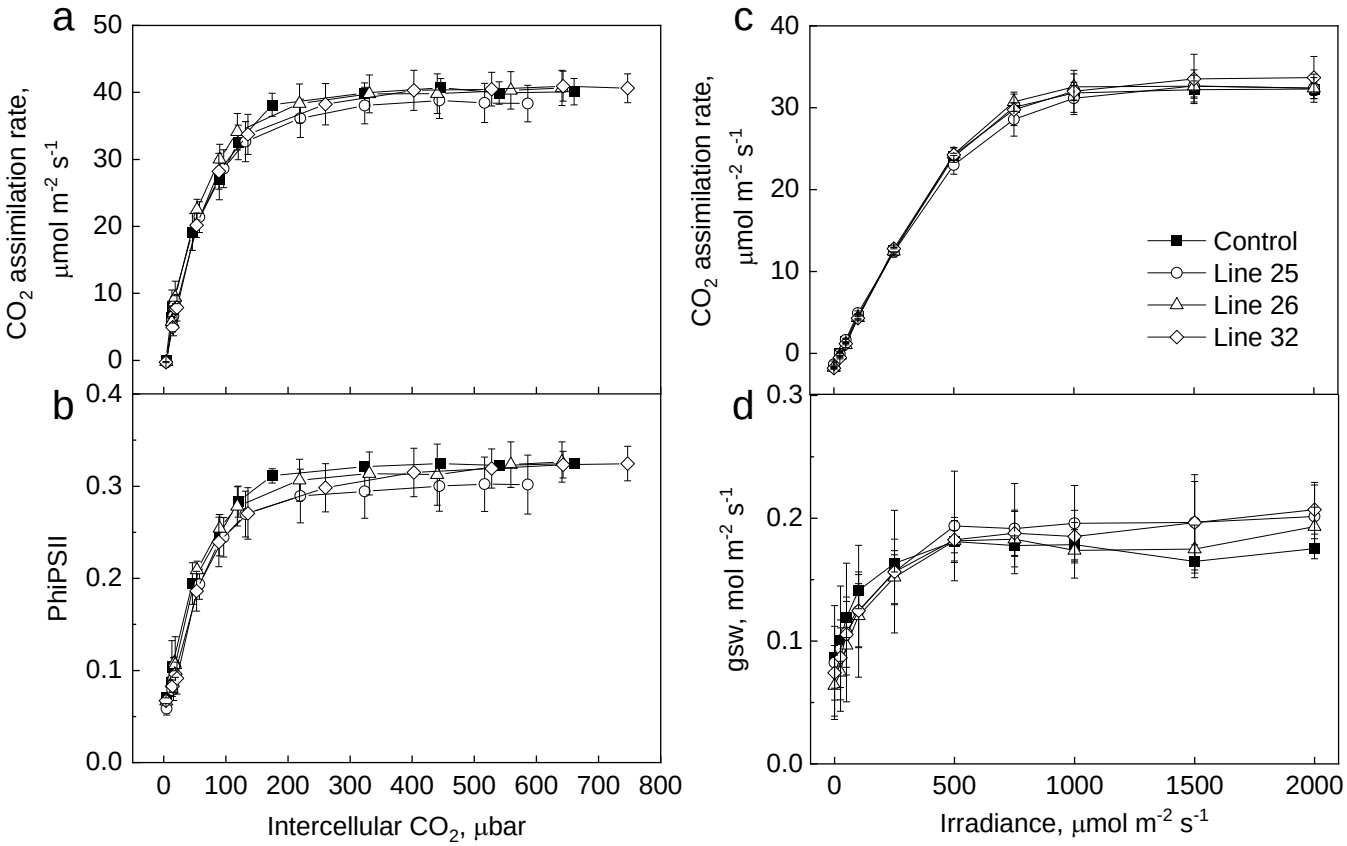

411

412 **Fig. 3.** Gas exchange and fluorescence analysis of control and transgenic sorghum plants overexpressing
413 Rieske at different pCO_2 (left panels, measured at 1500 μmol photons m^{-2} s^{-1}) or irradiance (right panels,
414 measured at ambient pCO_2). PhiPSII, the effective quantum yield of PSII; gsw, stomatal conductance to
415 water vapor. Azygous plants were used as control. Mean ± SE, n = 5 biological replicates. No statistically
416 significant differences were found between transgenic and control plants (one-way ANOVA and Dunnett's
417 post-hoc test at $P < 0.05$).

418

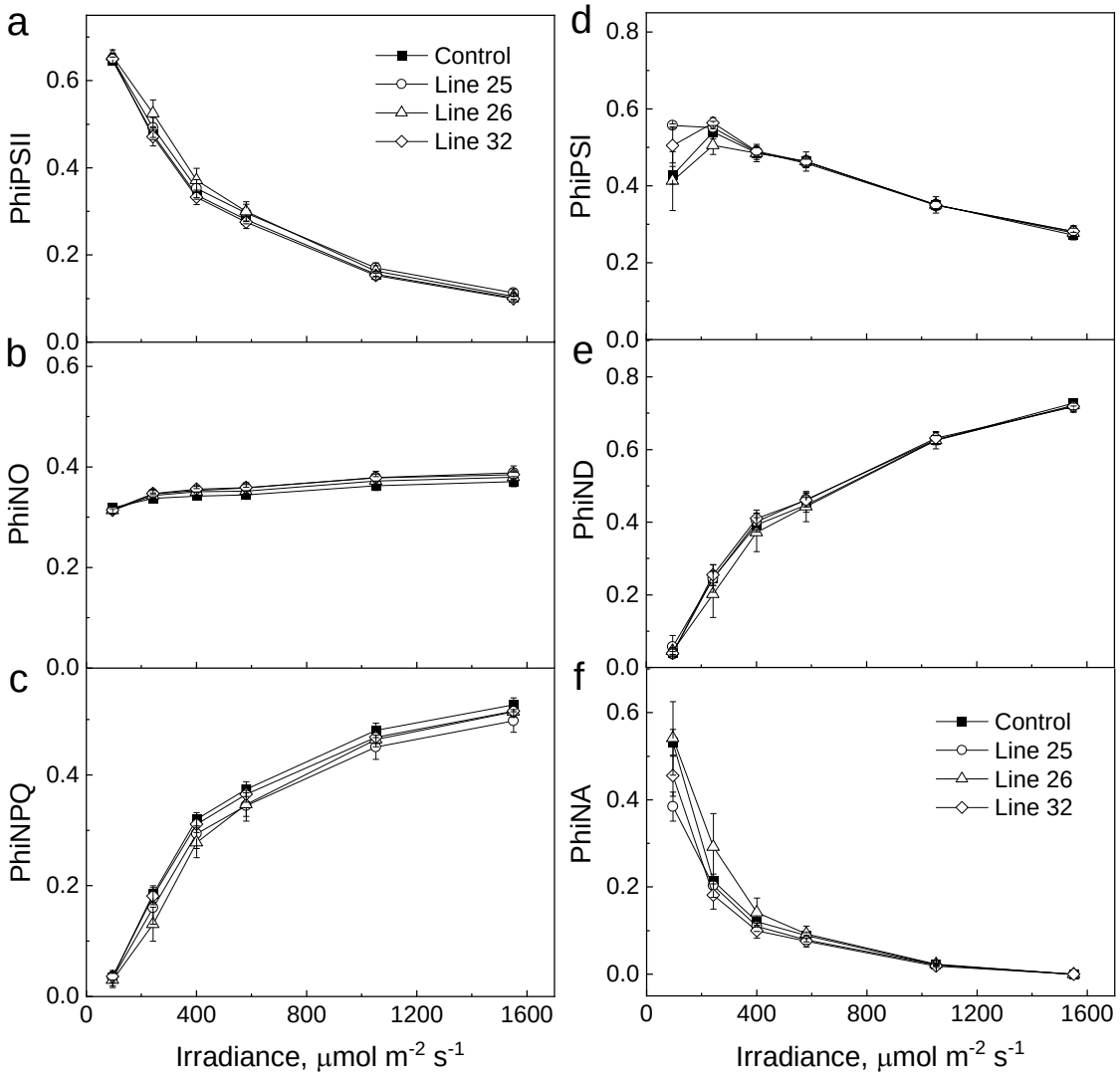

419

420 **Fig. 4.** Electron transport parameters estimated at different irradiance from leaves of control and transgenic
421 sorghum plants overexpressing Rieske. PhiPSII, the effective quantum yield of PSII; PhiNPQ, the yield of
422 non-photochemical quenching; PhiNO, the yield of non-regulated non-photochemical reactions within PSII;
423 PhiPSI, the effective quantum yield of PSI; PhiND, the non-photochemical yield of PSI due to the donor side
424 limitation; PhiNA, the non-photochemical yield of PSI due to the acceptor side limitation. Azygous plants
425 were used as control. Mean ± SE, *n* = 5 biological replicates. Asterisks indicate statistically significant
426 difference between line 25 (black) or line 32 (grey) and control plants (one-way ANOVA and Dunnett's post-
427 hoc test at $P < 0.05$).

428

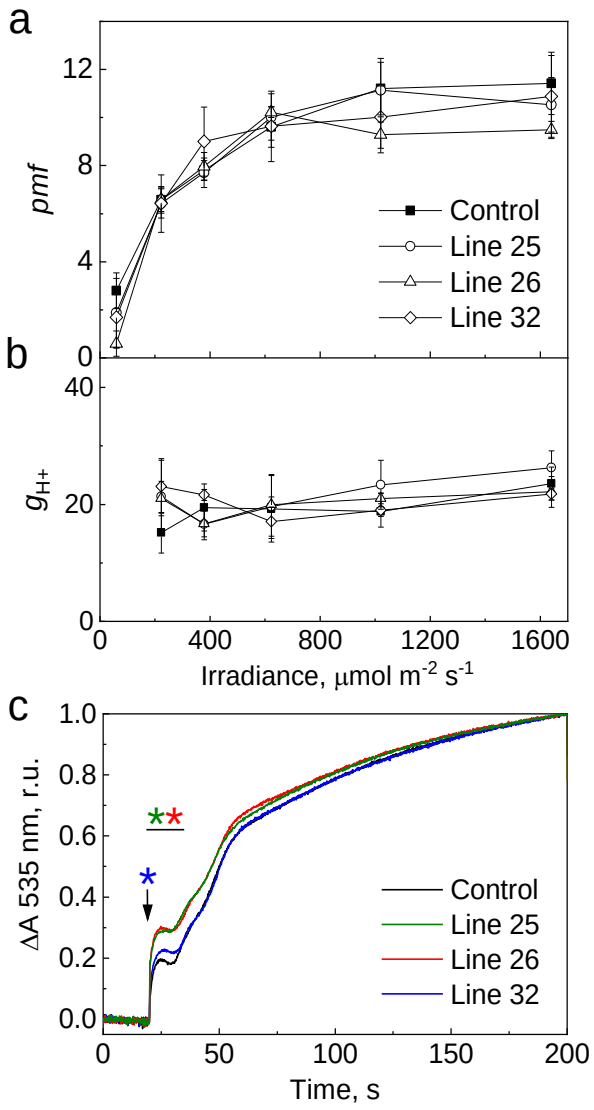

Fig. 5. Analysis of the thylakoid membrane energisation in control plants and transgenic sorghum lines overexpressing Rieske. (**a** and **b**) Proton motive force (*pmf*) and proton conductivity of the thylakoid membrane (g_{H+}) at different irradiance analysed using electrochromic shift signal. Mean ± SE, n = 4 biological replicates. **c**. Absorbance changes at 535 nm recorded upon the shift from dark to 1600 μmol m^{-2} s^{-1}. The absorbance at the beginning and end of the 3-min illumination period was normalised to 0 and 1, respectively, to facilitate comparison of the kinetics. Averages of 4 biological replicates are presented. Azygous plants were used as control. Asterisks indicate intervals of statistically significant difference between transgenic and control plants (one-way ANOVA and Dunnett's post-hoc test at $P < 0.05$).

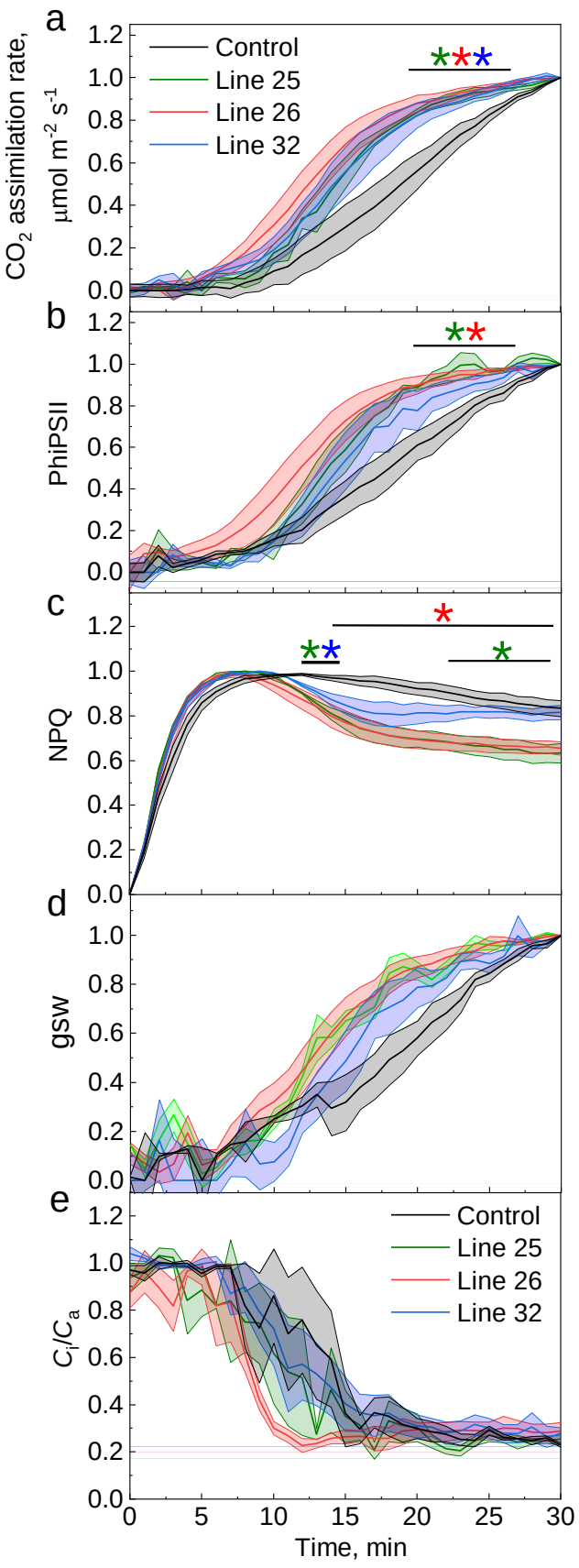

Fig. 6. Induction of photosynthesis during the first 30 min of illumination with actinic light of 1000 µmol m^{-2} s^{-1} in control plants and transgenic sorghum lines overexpressing Rieske. PhiPSII, the effective quantum yield of PSII; NPQ, non-photochemical quenching; gsw, stomatal conductance to water vapor; C_i/C_a, the ratio between the intercellular and ambient CO_2 partial pressures. The values of each parameter, except for C_i/C_a, at the beginning and end of the 30-min illumination were normalised to 0 and 1, respectively, to facilitate comparison of the kinetics. Azygous plants were used as control. Mean ± SE, n = 5 biological replicates. Asterisks indicate intervals of statistically significant differences between transgenic and control plants (one-way ANOVA and Dunnett's post-hoc test at $P < 0.05$).

Supplementary figures

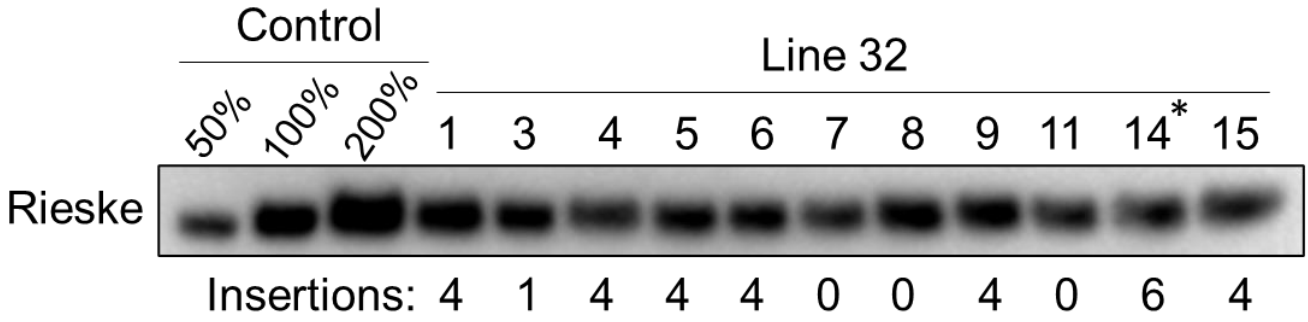

Fig. S1. Immunodetection of Rieske in the T_1 progeny of line 32. Samples were loaded on leaf area basis, and the WT sample was used as a control. Insertion numbers indicate a copy number of *ntpII* obtained by digital PCR. Asterisk indicates homozygous plant 32-14 which T_2 progeny was used in further experiments.

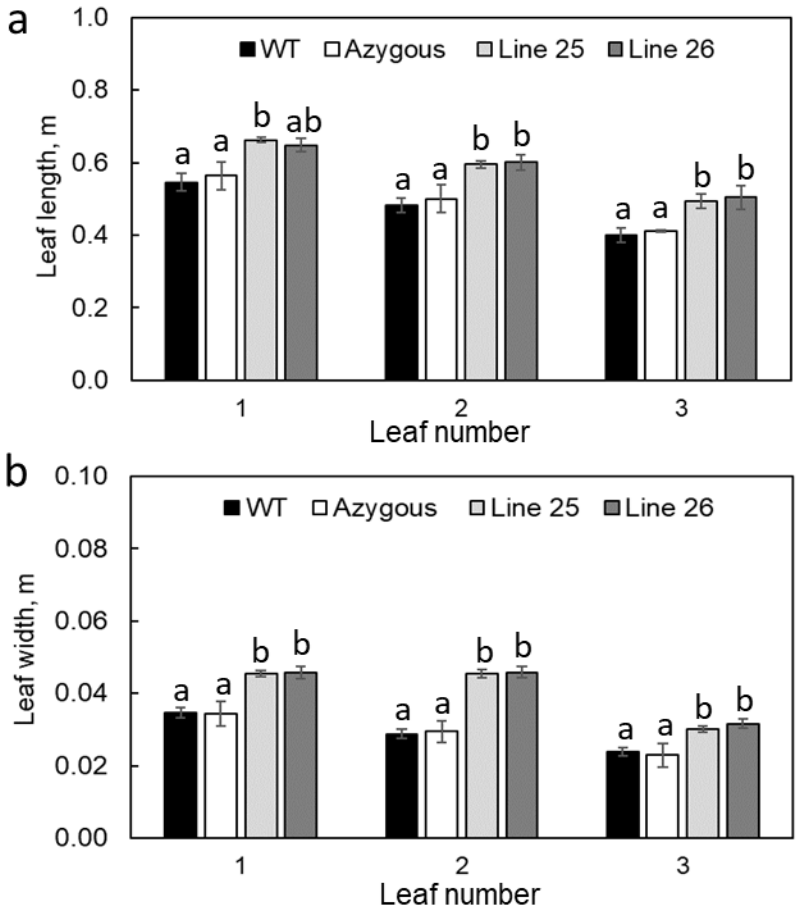

Fig. S2. Length and width of top fully expanded leaves from WT, azygous and Rieske overexpressing plants. Mean ± SE, *n* = 5 biological replicates. Letters indicate statistically significant differences between groups (one-way ANOVA and Tukey post-hoc test, $P < 0.05$).

References

Acevedo-Siaca, L.G., Coe, R., Wang, Y., Kromdijk, J., Quick, W.P. and Long, S.P. (2020) Variation in photosynthetic induction between rice accessions and its potential for improving productivity. *New Phytologist* **227**, 1097-1108.

Alonso-Cantabrana, H., Cousins, A.B., Danila, F., Ryan, T., Sharwood, R.E., von Caemmerer, S. and Furbank, R.T. (2018) Diffusion of CO_2 across the mesophyll-bundle sheath cell interface in a C_4 plant with genetically reduced PEP carboxylase activity. *Plant Physiology* **178**, 72-81.

Ananda, G.K.S., Myrans, H., Norton, S.L., Gleadow, R., Furtado, A. and Henry, R.J. (2020) Wild Sorghum as a promising resource for crop improvement. *Frontiers in Plant Science* **11**.

Bellasio, C. and Ermakova, M. (2021) Resolving leaf level metabolism of C_4 *Setaria viridis* acclimated to low light through a biochemical model. *bioRxiv*.

Bellasio, C. and Lundgren, M.R. (2016) Anatomical constraints to C_4 evolution: light harvesting capacity in the bundle sheath. *New Phytologist* **212**, 485–496.

Bilger, W. and Björkman, O. (1990) Role of the xanthophyll cycle in photoprotection elucidated by measurements of light-induced absorbance changes, fluorescence and photosynthesis in leaves of *Hedera canariensis*. *Photosynthesis Research* **25**, 173-185.

Craufurd, P.Q. and Peacock, J.M. (1993) Effect of heat and drought stress on sorghum (*Sorghum bicolor*). II. Grain yield. *Exp. Agric.* **29**, 77-86.

Deans, R.M., Farquhar, G.D. and Busch, F.A. (2019) Estimating stomatal and biochemical limitations during photosynthetic induction. *Plant, Cell & Environment* **42**, 3227-3240.

Edwards, G.E., Furbank, R.T., Hatch, M.D. and Osmond, C.B. (2001) What does it take to be C_4? Lessons from the evolution of C_4 photosynthesis. *Plant Physiology* **125**, 46-49.

Engler, C., Youles, M., Gruetzner, R., Ehnert, T.-M., Werner, S., Jones, J.D.G., Patron, N.J. and Marillonnet, S. (2014) A Golden Gate modular cloning toolbox for plants. *ACS Synthetic Biology* **3**, 839-843.

Ermakova, M., Bellasio, C., Fitzpatrick, D., Furbank, R., Mamedov, F. and von Caemmerer, S. (2021a) Upregulation of bundle sheath electron transport capacity under limiting light in C_4 *Setaria viridis*. *The Plant Journal* **106**, 1443-1454.

Ermakova, M., Lopez-Calcagno, P.E., Furbank, R.T., Raines, C.A. and von Caemmerer, S. (2022) Increased sedoheptulose-1,7-bisphosphatase content in the C_4 *Setaria viridis* does not affect photosynthesis. *bioRxiv* **doi:10.1101/2022.05.09.491242**.

Ermakova, M., Lopez-Calcagno, P.E., Raines, C.A., Furbank, R.T. and von Caemmerer, S. (2019) Overexpression of the Rieske FeS protein of the Cytochrome b_6f complex increases C_4 photosynthesis in *Setaria viridis*. *Communications Biology* **2**.

Ermakova, M., Osborn, H., Groszmann, M., Bala, S., Bowerman, A., McGaughey, S., Byrt, C., Alonso-cantabrana, H., Tyerman, S., Furbank, R.T., Sharwood, R.E. and von Caemmerer, S. (2021b) Expression of a CO_2-permeable aquaporin enhances mesophyll conductance in the C_4 species *Setaria viridis*. *Elife* **10**, e70095.

Furbank, R.T. (2011) Evolution of the C_4 photosynthetic mechanism: are there really three C_4 acid decarboxylation types? *Journal of Experimental Botany* **62**, 3103-3108.

Furbank, R.T. and Hatch, M.D. (1987) Mechanism of C_4 photosynthesis - the size and cof the inorganic carbon pool in bundle sheath-cells. *Plant Physiology* **85**, 958-964.

Furbank, R.T. and Taylor, W.C. (1995) Regulation of photosynthesis in C_3 and C_4 plants: a molecular approach. *The Plant Cell* **7**, 797-807.

Furbank, R.T. and Walker, D.A. (1985) Photosynthetic induction in C_4 leaves. *Planta* **163**, 75-83.

Genty, B., Briantais, J.M. and Baker, N.R. (1989) The relationship between the quantum yield of photosynthetic electron-transport and quenching of chlorophyll fluorescence. *Biochimica Et Biophysica Acta* **990**, 87-92.

Gurel, S., Gurel, E., Kaur, R., Wong, J., Meng, L., Tan, H.-Q. and Lemaux, P.G. (2009) Efficient, reproducible Agrobacterium-mediated transformation of sorghum using heat treatment of immature embryos. *Plant Cell Reports* **28**, 429-444.

Hatch, M.D. (1987) C_4 photosynthesis - a unique blend of modified biochemistry, anatomy and ultrastructure. *Biochimica Et Biophysica Acta* **895**, 81-106.

Heyno, E., Ermakova, M., Lopez-Calcagno, P.E., Woodford, R., Brown, K.L., Matthews, J.S.A., Osmond, B., Raines, C.A. and Caemmerer, S.v. (2022) Rieske FeS overexpression in tobacco provides increased abundance and activity of Cytochrome b_6f. *bioRxiv*, doi: 2022.2006.2028.497970.

Horton, P., Ruban, A.V., Rees, D., Pascal, A.A., Noctor, G. and Young, A.J. (1991) Control of the light-harvesting function of chloroplast membranes by aggregation of the LHCII chlorophyll—protein complex. *FEBS Letters* **292**, 1-4.

Hu, H., Mauro-Herrera, M. and Doust, A.N. (2018) Domestication and improvement in the model C_4 grass, Setaria. *Frontiers in Plant Science* **9**.

Ishikawa, N., Takabayashi, A., Sato, F. and Endo, T. (2016) Accumulation of the components of cyclic electron flow around Photosystem I in C_4 plants, with respect to the requirements for ATP. *Photosynthesis Research*, 1-17.

Johnson, G.N. (2011) Physiology of PSI cyclic electron transport in higher plants. *Biochimica Et Biophysica Acta-Bioenergetics* **1807**, 384-389.

Johnson, M.P., Pérez-Bueno, M.L., Zia, A., Horton, P. and Ruban, A.V. (2009) The zeaxanthin-independent and zeaxanthin-dependent qE components of nonphotochemical quenching involve common conformational changes within the photosystem II antenna in Arabidopsis. *Plant physiology* **149**, 1061-1075.

Kanai, R. and Edwards, G.E. (1999) The biochemistry of C_4 photosynthesis. In: *C_4 plant biology* (Sage, R.F. and Monson, R.K. eds). San Diego: Academic Press.

Kanazawa, A. and Kramer, D.M. (2002) In vivo modulation of nonphotochemical exciton quenching (NPQ) by regulation of the chloroplast ATP synthase. *Proceedings of the National Academy of Sciences* **99**, 12789-12794.

Klughammer, C. and Schreiber, U. (2008) Saturation pulse method for assessment of energy conversion in PS I. *PAM Application notes* **1**, 3.

Kramer, D., Johnson, G., Kiirats, O. and Edwards, G. (2004) New fluorescence parameters for the determination of QA redox state and excitation energy fluxes. *Photosynthesis Research* **79**, 209-218.

Kromdijk, J., Głowacka, K., Leonelli, L., Gabilly, S.T., Iwai, M., Niyogi, K.K. and Long, S.P. (2016) Improving photosynthesis and crop productivity by accelerating recovery from photoprotection. *Science* **354**, 857-861.

Kromdijk, J., Griffiths, H. and Schepers, H.E. (2010) Can the progressive increase of C_4 bundle sheath leakiness at low PFD be explained by incomplete suppression of photorespiration? *Plant Cell and Environment* **33**, 1935-1948.

Kromdijk, J., Ubierna, N., Cousins, A.B. and Griffiths, H. (2014) Bundle-sheath leakiness in C_4 photosynthesis: a careful balancing act between CO_2 concentration and assimilation. *Journal of Experimental Botany* **65**, 3443-3457.

Kuhlgert, S., Austic, G., Zegarac, R., Osei-Bonsu, I., Hoh, D., Chilvers Martin, I., Roth Mitchell, G., Bi, K., TerAvest, D., Weebadde, P. and Kramer David, M. (2016) MultispeQ Beta: a tool for large-scale plant phenotyping connected to the open PhotosynQ network. *Royal Society Open Science* **3**, 160592.

Li, X.-P., Gilmore, A.M., Caffarri, S., Bassi, R., Golan, T., Kramer, D. and Niyogi, K.K. (2004) Regulation of photosynthetic light harvesting involves intrathylakoid lumen pH sensing by the PsbS protein. *Journal of Biological Chemistry* **279**, 22866-22874.

Li, X.-P., Müller-Moulé, P., Gilmore Adam, M. and Niyogi Krishna, K. (2002) PsbS-dependent enhancement of feedback de-excitation protects photosystem II from photoinhibition. *Proceedings of the National Academy of Sciences* **99**, 15222-15227.

Long, S.P. (1999) Environmental responses. *C_4 plant biology*, 215-249.

Long, S.P., Taylor, S.H., Burgess, S.J., Carmo-Silva, E., Lawson, T., De Souza, A.P., Leonelli, L. and Wang, Y. (2022) Into the shadows and back into sunlight: photosynthesis in fluctuating light. *Annual Review of Plant Biology* **73**, 617-648.

Malnoë, A. (2018) Photoinhibition or photoprotection of photosynthesis? Update on the (newly termed) sustained quenching component qH. *Environmental and Experimental Botany* **154**, 123-133.

Malone, L.A., Proctor, M.S., Hitchcock, A., Hunter, C.N. and Johnson, M.P. (2021) Cytochrome b6f – orchestrator of photosynthetic electron transfer. *Biochimica et Biophysica Acta (BBA) - Bioenergetics* **1862**, 148380.

Müller, P., Li, X.-P. and Niyogi, K.K. (2001) Non-photochemical quenching. A response to excess light energy. *Plant physiology* **125**, 1558-1566.

Munekage, Y. (2016) Light harvesting and chloroplast electron transport in NADP-malic enzyme type C_4 plants. *Current Opinion in Plant Biology* **31**, 9-15.

Munekage, Y. and Taniguchi, Y.Y. (2016) Promotion of cyclic electron transport around Photosystem I with the development of C_4 photosynthesis. *Plant and Cell Physiology* **57**, 897-903.

Nakamura, N., Iwano, M., Havaux, M., Yokota, A. and Munekage, Y.N. (2013) Promotion of cyclic electron transport around photosystem I during the evolution of NADP–malic enzyme-type C_4 photosynthesis in the genus *Flaveria*. *New Phytologist* **199**, 832-842.

Osborn, H.L., Evans, J.R., Sharwood, R.E., Furbank, R.T., von Caemmerer, S., Alonso-Cantabrana, H. and Covshoff, S. (2016) Effects of reduced carbonic anhydrase activity on CO_2 assimilation rates in *Setaria viridis*: a transgenic analysis. *Journal of Experimental Botany* **68**, 299-310.

Otani, T., Kato, Y. and Shikanai, T. (2018) Specific substitutions of light-harvesting complex I proteins associated with photosystem I are required for supercomplex formation with chloroplast NADH dehydrogenase-like complex. *The Plant Journal* **94**, 122-130.

Pignon, C.P. and Long, S.P. (2020) Retrospective analysis of biochemical limitations to photosynthesis in 49 species: C_4 crops appear still adapted to pre-industrial atmospheric [CO_2]. *Plant, Cell & Environment* **43**, 2606-2622.

Sacksteder, C.A. and Kramer, D.M. (2000) Dark-interval relaxation kinetics (DIRK) of absorbance changes as a quantitative probe of steady-state electron transfer. *Photosynthesis Research* **66**, 145.

Sage, R.F., Christin, P.-A. and Edwards, E.J. (2011) The C_4 plant lineages of planet Earth. *Journal of Experimental Botany* **62**, 3155-3169.

Sage, R.F. and Zhu, X.-G. (2011) Exploiting the engine of C_4 photosynthesis. *Journal of Experimental Botany* **62**, 2989-3000.

Sales, C.R.G., Wang, Y., Evers, J.B. and Kromdijk, J. (2021) Improving C_4 photosynthesis to increase productivity under optimal and suboptimal conditions. *Journal of Experimental Botany* **72**, 5942-5960.

Salesse-Smith, C.E., Sharwood, R.E., Busch, F.A., Kromdijk, J., Bardal, V. and Stern, D.B. (2018) Overexpression of Rubisco subunits with RAF1 increases Rubisco content in maize. *Nature Plants* **4**, 802-810.

Slattery, R.A., Walker, B.J., Weber, A.P.M. and Ort, D.R. (2018) The impacts of fluctuating light on crop rerformance. *Plant Physiology* **176**, 990-1003.

Tao, Y., George-Jaeggli, B., Bouteillé-Pallas, M., Tai, S., Cruickshank, A., Jordan, D. and Mace, E. (2020a) Genetic diversity of C_4 photosynthesis pathway genes in *Sorghum bicolor* (L.). *Genes* **11**.

Tao, Y., Zhao, X., Wang, X., Hathorn, A., Hunt, C., Cruickshank, A.W., van Oosterom, E.J., Godwin, I.D., Mace, E.S. and Jordan, D.R. (2020b) Large-scale GWAS in sorghum reveals common genetic control of grain size among cereals. *Plant Biotechnology Journal* **18**, 1093-1105.

Usuda, H. and Edwards, G.E. (1984) Is photosynthesis during the induction period in maize limited by the availability of intercellular carbon dioxide? *Plant Science Letters* **37**, 41-45.

van Oosterom, E.J. and Hammer, G.L. (2008) Determination of grain number in sorghum. *Field Crops Research* **108**, 259-268.

von Caemmerer, S. (2000) *Biochemical models of leaf photosynthesis*. Collingwood:CSIRO Publishing.

von Caemmerer, S. (2021) Updating the steady state model of C_4 photosynthesis. *Journal of Experimental Botany* **72**, 6003-6017.

von Caemmerer, S. and Furbank, R.T. (1999) Modelling C_4 photosynthesis. In: *The biology of C_4 photosynthesis* (Sage, R.F. and Monson, R.K. eds), pp. 173-211. London: Academic Press.

von Caemmerer, S. and Furbank, R.T. (2016) Strategies for improving C_4 photosynthesis. *Current Opinion in Plant Biology* **31**, 125-134.

Wang, Y., Chan, K.X. and Long, S.P. (2021) Towards a dynamic photosynthesis model to guide yield improvement in C_4 crops. *The Plant Journal* **107**, 343-359.

Wu, A., Hammer, G.L., Doherty, A., von Caemmerer, S. and Farquhar, G.D. (2019) Quantifying impacts of enhancing photosynthesis on crop yield. *Nature Plants* **5**, 380-388.

Zhu, W., Xu, J., Chen, S., Chen, J., Liang, Y., Zhang, C., Li, Q., Lai, J. and Li, L. (2021) Large-scale translatome profiling annotates the functional genome and reveals the key role of genic 3' untranslated regions in translatomic variation in plants. *Plant Communications* **2**, 100181.